

# SHAPE OPTIMIZATION PROBLEMS WITH RANDOM COEFFICIENTS VIA THE PENALTY METHOD

XIAOWEI PANG

**ABSTRACT.** For shape optimization problems, governed by elliptic equations with Dirichlet boundary condition and random coefficients, we utilize a penalization technique to get the approximate problem. We consider that uncertainties exist in the diffusion coefficients and minimize objective functions in mean value form. Finite element method, Monte Carlo method and accelerated version of the gradient descent method are applied to solve the corresponding discretized problem. The convergence analysis and numerical results are included.

**Keywords:** shape optimization; penalization; random coefficients; finite element method.

**MSC(2020):** 35R60, 49Q10, 49M25, 65M60

## 1. INTRODUCTION

Shape and topology optimization have emerged as pivotal tools in engineering design [24, 28, 30]. They systematically improve structural performance under given constraints, such as minimizing compliance, maximizing stiffness, or enhancing reliability. Modeling physical phenomena via partial differential equations (PDEs) is central to this process. Elliptic PDEs are key tool for describing equilibrium states in solid mechanics, heat transfer, and fluid flow [2, 6, 21]. However, real-world systems exhibit inherent uncertainties. These arise from material properties, applied loads, or geometric variations. Such uncertainties render deterministic PDE models insufficient. Consequently, shape optimization problems constrained by stochastic elliptic PDEs, where randomness is incorporated into coefficients, source terms, or boundary data, attracts significant interest [11, 16, 17].

In this work, we concentrate on solving stochastic shape optimization problem constrained by random elliptic PDEs, in which the optimization variable is deterministic, and state variable is uncertain, by minimizing the expected value of the

---

Corresponding Author: Xiaowei Pang (pangxw21@hebtu.edu.cn).

cost functional over all random parameters. We utilize the discretize-then-optimize framework to achieve our aim [14].

A key challenge in shape optimization lies in handling the dynamic nature of the domain. As the shape or topology evolves, the computational mesh must adapt. This adaption causes remeshing difficulties, numerical instability, and increased computational cost. To address this, penalty methods for the constraint equation and cost functional have gained prominence [15, 20, 22, 25, 26]. These methods map the evolving physical domain onto a fixed reference domain. They introduce a level set function to represent shape or topology changes within a static computational framework. By avoiding mesh deformation or regeneration, it simplifies the implementation of numerical schemes. This simplification is especially useful when coupled with finite element discretizations of PDEs. The approach is particularly advantageous for problems with homogeneous boundary conditions—such as Dirichlet or Neumann conditions with zero values on fixed boundaries. Here, the fixed domain can be preprocessed to enforce boundary constraints consistently across all design iterations [22, 23]. In [4], Bogosel generated the discrete convex shape with the aid of support function or the gauge function. Chakib et al. solved the shape optimization problem governed by Laplace or Stokes operator using the Minkowski deformation of convex domain [5]. Other numerical methods include multigrid method, continuity preserving discrete shape gradient method, level set method, and neural work method, the reader can refer to [1, 9, 18, 31].

Coupling randomness with shape optimization in stochastic elliptic PDEs adds significant complexity. Uncertainties in, for instance, the diffusion coefficient or the source term of the elliptic equation propagate the solution. This propagation affects the objective function, like expected compliance or failure probability. Approaches to handle such uncertainties, include using deterministic approximations. Such as [2] applied Taylor expansions to the cost function with respect to random variables. These approximations reduce the computational burden and make stochastic shape optimization feasible. Conti et al. studied risk averse elasticity optimization problem based on a regularized gradient flow in [7], they minimized a nonlinear monotone increasing function of the objective function to replace the expectation of the objective function. More literature on random shape optimization problems can be found in [8, 10, 11, 17, 19]. Beyond that, Monte Carlo simulations, although often suffer from high computational cost, but can be applied to almost

any complex problem, especially excelling in handling high-dimensional integrals, complex stochastic systems, and probability calculations. Besides, the computations of different samples are completely independent, which can perfectly utilize parallel computing resources and achieve efficient acceleration.

Ultimately, in shape optimization problems, most studies employ gradient descent or quasi-Newton algorithms. These algorithms leverage shape derivatives to guide design updates. For example, Martínez-Frutos et al. computed sensitivities of the objective function with respect to shape perturbations to drive robust optimal design, [17]. In [4], Bogosel used gradient-based approaches for numerical shape optimization among convex sets, ensuring convergence within convex design spaces. Chakib et al. designed numerical approaches—augmented Lagrangian and adaptive schemes to handle constraints in convex domain shape optimization, improving efficiency and convergence [5].

This paper is organized as follows. In Section 2, we recall some basic definitions, preliminaries about random shape optimization problem, and present the convergence result under some conditions. Moving on to Section 3, we propose the numerical algorithm. Some numerical examples are reported in Section 4. Finally, Section 5 gives the conclusion.

## 2. RPDES-CONSTRAINED OPTIMAL SHAPE PROBLEM

**2.1. Preliminaries.** For the convenience of subsequent descriptions, we present some notions and definitions firstly. Let  $D$  is a fixed convex bounded connected polygonal domain in  $\mathbb{R}^2$ ,  $v$  is a measurable function, following the symbols used in [14], the Lebesgue integration function space on  $D$  can be defined by

$$L^p(D) := \{v \mid \|v\|_{L^p(D)} < \infty, 1 \leq p \leq \infty\}$$

with

$$\begin{aligned} \|v\|_{L^p(D)} &= \left( \int_D |v(x)|^p dx \right)^{\frac{1}{p}}, \quad p \in [1, \infty), \\ \|v\|_{L^\infty(D)} &= \operatorname{ess\,sup}_{x \in D} |v(x)| = \inf\{\alpha \geq 0, \mu(\{|v(x)| > \alpha\}) = 0\}, \end{aligned}$$

where  $\mu(\cdot)$  stands for the measure. Therefore, the corresponding Sobolev space could be described by

$$W^{m,p}(D) = \{v \mid D^\alpha(v) \in L^p(D), |\alpha| \leq m\}$$

with the norm

$$\|v\|_{W^{m,p}} = \left( \sum_{|\alpha| \leq m} \|D^\alpha v\|_{L^p(D)}^p \right)^{1/p}, \quad p \in [1, \infty),$$

$$\|v\|_{W^{m,\infty}(D)} = \sum_{|\alpha| \leq m} \|D^\alpha v\|_{L^\infty(D)}.$$

Here,  $D^\alpha v$  stands for the weak derivative of  $v$ . Further, it is not difficult to find that  $H^k(D) = W^{k,2}(D)$  is a Hilbert space with the inner product

$$(u, v)_{H^m(D)} = \sum_{|\alpha| \leq m} (D^\alpha u, D^\alpha v)_{L^2(D)}.$$

Next, let  $H_0^m(D) = W_0^{m,2}(D)$  denotes the closure of  $C_0^\infty(D)$  in  $W^{m,2}(D)$ , and  $H^{-1}(D) = (H_0^1(D))^*$  be the dual space of  $H_0^1(D)$ . Applying Poincaré's inequality [29], there must exist a Poincaré constant  $C_p$  such that

$$(1) \quad |v|_{H^1(D)} \leq \|v\|_{H^1(D)} \leq C_p |v|_{H^1(D)}, \quad \forall v \in H_0^1(D),$$

where  $|v|_{H^1(D)} = \int_D |\nabla v|^2 dx$ .

The Bochner function space should be introduced as follows:

$$L^p(\Gamma; H) = \left\{ v \mid \int_\Gamma \|v(\cdot, \omega)\|_H^p dP < +\infty \right\},$$

where  $v(\cdot, \omega)$  is measurable function from  $\Gamma$  to  $H$  with the measure space  $(\Gamma, \mathcal{F}, P)$ , and  $H$  is a Hilbert function space, the norm of Bochner spaces is denoted by

$$\|v\|_{L^p(\Gamma; H)} = \left( \int_\Gamma \|v(\cdot, \omega)\|_H^p dP \right)^{\frac{1}{p}}, \quad 1 \leq p < \infty.$$

At the end of this subsection, we introduce Hedberg–Keldys stability property for domains of class  $C$ , [21, see Chapter 2 ].

**Lemma 2.1.** *If  $\Omega$  is an open bounded set of class  $C$ ,  $z \in H^1(\mathbb{R}^d)$  and  $z = 0$  almost everywhere in  $\mathbb{R}^d \setminus \Omega$ , then  $z \in H_0^1(\Omega)$ .*

**2.2. Statement of shape optimization problem.** Based on the notations defined in Subsection 2.1, the problems of interest are shape optimization problem constrained by random elliptic PDEs (RPDEs):

$$(2) \quad \min_K \mathbb{E} \left[ \int_\Omega J(x, \omega, u(x, \omega)) \right]$$

$$(3) \quad -\nabla \cdot (\alpha(x, \omega) \nabla u(x, \omega)) = f(x), \quad \text{in } K,$$

$$(4) \quad u(x, \omega) = 0, \quad \text{on } \partial K.$$

Here,  $K$  is unknown domain with  $K \subset D \subset \mathbb{R}^d$  or there exists a given open bounded set  $O$  such that  $O \subset K \subset D \subset \mathbb{R}^d$ , and  $\Omega$  is a integration domain, it could be the domain  $K$ ,  $O$ . Besides, state variable  $u \in U = L^2(\Gamma; H_0^1(D))$ , and right-hand side term  $f \in F = L^2(D)$  is a deterministic function. The notation  $\mathbb{E}$  denotes the expectation operator defined by  $\mathbb{E}[z(\omega)] = \int_{\Gamma} z(\omega) dP$ , where  $\omega$  is a random variable of probability space  $(\Gamma, \mathcal{F}, P)$ . The function  $J(\cdot, \cdot, \cdot)$  is some measurable and continuous Carathéodory mapping. For example, in ‘optimal layout’ problem,  $J = \|y - y_d\|^2$ , and  $y_d \in L^2(D)$  is a given function [21, Chapter 5], while  $J = a(x)\|y - y_d\|^2 + b(x)\|\nabla y - z_d\|^2$  in tomography problem, where  $a(x), b(x) \in L_+^\infty(D)$  and  $z_d \in L^2(D)^d$  are given functions [23].

The main difference between the studied model here and the traditional shape optimization problem is the constraint PDE, which has an uncertainty coefficient  $\alpha(x, \omega)$ .

Under the following assumption on  $\alpha$ , applying Lax-Milgram theorem and Poincaré inequality, it leads to the conclusion that the constraint stochastic PDE is well-posed for almost all  $\omega \in \Gamma$ .

**Assumption 2.2.** (cf. [12]) *For all  $(x, \omega) \in D \times \Gamma$ , there exists  $0 < \alpha_{min} < \alpha_{max} < \infty$ , such that*

$$(5) \quad 0 < \alpha_{min} \leq \alpha(x, \omega) \leq \alpha_{max} < \infty.$$

The variational form of the constraint, the stochastic PDE is: find  $u \in U$  satisfies

$$(6) \quad \mathbb{E} [\bar{a}(u, v; \omega)] = \mathbb{E} [l(f, v)], \quad \forall v \in U,$$

where  $\bar{a}(u, v; \omega) = (\alpha(x, \omega) \nabla u, \nabla v)_{L^2(D)}$  and  $l(f, v) = (f, v)_{L^2(D)}$ . For any  $\omega \in \Gamma$ , it is easy to see that  $\bar{a} : U \times U \rightarrow \mathbb{R}$  and  $l : F \times U \rightarrow \mathbb{R}$  are all continuous bilinear functionals.

**Lemma 2.3.** (cf. [27]) *Under the assumption 2.2, the stochastic elliptic equations admit a unique solution  $u \in L^2(\Gamma; H_0^1(D))$  which has the following estimate*

$$(7) \quad \|u(\cdot, \omega)\|_{L^2(D)} \leq C_1 \|f\|_{L^2(D)}, \quad \text{for a.e. } \omega \in \Gamma,$$

where  $C_1 = \frac{C_p}{\alpha_{min}}$  is a constant.

**2.3. Approximation problem.** We first parametrize the set  $K$  by a continuous function  $g$ , so that  $K$  can be denoted by

$$(8) \quad K = K_g = \text{int}\{x \in D \mid g(x) \geq 0\},$$

it is not necessarily connected,  $g \in C(\bar{D})$  is the corresponding unknown parameterization, not uniquely determined by domain  $K$ .

Next, we add a penalty term on the constraint equation and define the approximation of state equation

$$(9) \quad -\nabla \cdot (\alpha(x, \omega) \nabla u_\epsilon(x, \omega)) + \frac{1}{\epsilon} (1 - H_\epsilon(g)) u_\epsilon(x, \omega) = f(x), \quad \text{in } D,$$

$$(10) \quad u_\epsilon(x, \omega) = 0, \quad \text{on } \partial D.$$

Here,  $\epsilon > 0$  is a penalty parameter and

$$H_\epsilon(g) = \begin{cases} 1, & g \geq 0, \\ \frac{(\epsilon - 2g)(g + \epsilon)^2}{\epsilon^3}, & -\epsilon < g < 0, \\ 0, & g \leq -\epsilon, \end{cases}$$

is a Lipschitz function.

Naturally, we can get the variational form of the approximate constraint equation: find  $u_\epsilon \in U$  such that

$$(11) \quad \mathbb{E}[a(u_\epsilon, v; \omega)] = \mathbb{E}[l(f, v)], \quad \forall v \in U,$$

where  $a(u_\epsilon, v; \omega) = (\alpha(x, \omega) \nabla u_\epsilon, \nabla v)_{L^2(D)} + \frac{1}{\epsilon} ((1 - H_\epsilon(g)) u_\epsilon, v)_{L^2(D)}$ .

Similar to Lemma 2.3, for any  $\omega \in \Gamma$ , the boundedness of  $H_\epsilon(g)$  can guarantee that the weak form is well-posed. Under appropriate assumptions on the domain  $K$ , we extend the result of the deterministic situation into a convergence result in the sense of expectation [23].

**Theorem 2.4.** *If  $K = K_g$  is Lipschitz domain, then there exists subsequences of  $\mathbb{E}[u_\epsilon]$  that weakly converge to  $\mathbb{E}[\bar{u}]$  in  $H^1(K_g)$  and strongly in  $L^2(K_g)$ .*

*Proof.* For any test function  $v = u_\epsilon(\cdot, \omega)$ , based on Poincaré inequality (1) and Assumption 2.2, we obtain

$$(12) \quad \alpha_{\min} \|u_\epsilon(\cdot, \omega)\|_{H_0^1(D)}^2 + \frac{1}{\epsilon} \int_D (1 - H_\epsilon(g)) u_\epsilon^2(\cdot, \omega) dx \leq \int_D f(x) u_\epsilon(\cdot, \omega) dx,$$

For all of the random variable, it yields

$$(13) \quad \alpha_{\min} \mathbb{E}[\|u_\epsilon\|^2] + \frac{1}{\epsilon} \int_\Gamma \int_D (1 - H_\epsilon(g)) u_\epsilon^2 dx dP \leq \int_\Gamma \int_D f(x) u_\epsilon dx dP.$$

It yields that  $\{u_\epsilon\}$  is bounded in  $U$ , due to the positivity of the penalization term. On one hand, we claim that  $\{\mathbb{E}[u_\epsilon]\}$  is bounded in  $H^1(K_g)$ , this is owing to  $K_g \subset D$  and

$$\|\mathbb{E}[u_\epsilon]\|_{H^1(K_g)} \leq \mathbb{E}[\|u_\epsilon\|_{H^1(D)}] \leq \sup_{\epsilon} \|u_\epsilon\|_U < \infty.$$

There exists a subsequence also denoted by  $\{\mathbb{E}[u_\epsilon]\}$ , which weakly converge to  $\mathbb{E}[\bar{u}]$  in  $H^1(K_g)$ .

On the other hand, since  $K_g$  is Lipschitz and it is also class  $C$ . As mentioned above,  $\{\mathbb{E}[u_\epsilon]\}$  is uniformly bounded in  $H^1(K_g)$ , by Rellich-Kondrachov theorem [3, Theorem 6.3, Remarks 6.4], then the embedding  $H^1(K_g) \rightarrow L^2(K_g)$  is compact and there exists a subsequence also noted by  $\mathbb{E}[u_\epsilon]$ , which strongly converges to some  $w \in L^2(K_g)$ . While the weakly convergence  $\mathbb{E}[u_\epsilon] \rightarrow \mathbb{E}[\bar{u}]$  holds in  $H^1(K_g)$ . By the uniqueness of the limit,  $w = \mathbb{E}[\bar{u}]$ , namely,  $\mathbb{E}[u_\epsilon] \rightarrow \mathbb{E}[\bar{u}]$  in  $L^2(K_g)$ , when  $\epsilon \rightarrow 0$ .

Furthermore,

$$\int_{\Gamma} \int_D (1 - H_\epsilon(g)) u_\epsilon^2 dx dP \rightarrow 0,$$

as  $\epsilon \rightarrow 0$ . Notice that function  $H_\epsilon(g), g$  are continuous,  $g(x) \leq 0$  holds in  $D \setminus K_g$ , so for sufficiently small  $\epsilon$ , any compact set  $S \subset D \setminus K_g$  and  $x \in S$ , there exists a constant  $r > 0$  enables  $g(x) \leq -r$  and  $H_\epsilon(g) = 0$  in the domain  $S$ . Thus, when  $\epsilon$  goes to 0,  $u_\epsilon$  also goes to 0 in  $L^2(\Gamma; L^2(S))$ , by the arbitrariness of  $S$ ,  $u_\epsilon \rightarrow 0$  in  $L^2(\Gamma; L^2(D \setminus K_g))$ , thereby  $\bar{u}(x, \omega) = 0$  holds a.e. in  $D \setminus K_g \times \Gamma$  and  $\mathbb{E}[\bar{u}] = 0$  a.e. in  $D \setminus K_g$ .

Moreover, for a.e.  $\omega \in \Gamma$ , by zero extension to  $\mathbb{R}^d \setminus D$ ,

$$\bar{u}(x, \omega) = \begin{cases} \bar{u}(x, \omega) & \text{if } x \in D, \\ 0 & \text{if } x \in \mathbb{R}^d \setminus D, \end{cases}$$

$D \setminus K_g \subset \mathbb{R}^d \setminus K_g$  illustrates  $\bar{u} = 0$  a.e. in  $\mathbb{R}^d \setminus K_g$ . Thus,  $\bar{u}(x, \omega) = 0$  a.e. in  $(\mathbb{R}^d \setminus K_g) \times \Gamma$ , combining Lemma 2.1 (with  $K_g$  of class  $C$ ) imply  $\bar{u}(\cdot, \omega) \in H_0^1(K_g)$ , hence  $\mathbb{E}[\bar{u}]|_{K_g} \in H_0^1(K_g)$ .

For any test function  $v \in L^2(\Gamma; C_0^\infty(K_g))$ ,  $H_\epsilon(g) = 1$ , and the approximate weak form is

$$(14) \quad \int_{\Gamma} \int_{K_g} \alpha(x, \omega) \nabla u_\epsilon \nabla v dx dP = \int_{\Gamma} \int_{K_g} f v dx dP,$$

when  $\epsilon$  tends to 0, the above equality indicates  $\mathbb{E}[\bar{u}]|_{K_g} \in H_0^1(K_g)$  is the weak solution of the original weak form (6).  $\square$

In (2), if

$$(15) \quad \int_{\Omega} J(x, \omega, u(x, \omega)) = \frac{1}{2} \int_K (u - u_d)^2 dx,$$

through similar discussion with [14], it is easy to get the weak form of dual or adjoint equation of (11): finding  $z \in U$ , such that

$$(16) \quad \int_{\Gamma} \int_D \left( \alpha(x, \omega) \nabla z \nabla v + \frac{1}{\epsilon} (1 - H_{\epsilon}(g)) z v \right) dx dP = \int_{\Gamma} \int_K (u - u_d) v dx dP, \quad \forall v \in U.$$

Under the consideration of the parametrization process, we can notice that (15) is equivalent to

$$(17) \quad \frac{1}{2} \int_D H_{\epsilon}(g) (u - u_d)^2 dx,$$

and the right-hand side of (16) can be replaced by  $\int_{\Gamma} \int_D H_{\epsilon}(g) (u - u_d) v dx dP$ .

**Remark 2.5.** *If*

$$(18) \quad \int_{\Omega} J(x, \omega, u(x, \omega)) = \frac{1}{2} \int_O (u - u_d)^2 dx,$$

*then the right-hand side of the dual weak form still is  $\int_{\Gamma} \int_O H_{\epsilon}(g) (u - u_d) v dx dP$  for the  $O$  is a given bounded region, it will not appear  $H_{\epsilon}(g)$ , and objective function is the same.*

Besides, the weak form (16) also has well-posedness. On account of the uniqueness of the weak solution, we can compute the gradient of the objective functional.

**Lemma 2.6.** *The stochastic approximate weak solution  $u_{\epsilon}(g, \omega)$  of (11) is Gâteaux differentiable about  $g$  from  $X(D)$  to  $L^2(\Gamma; H_0^1(D))$  and for any  $q \in X(D)$ ,  $y = \nabla u_{\epsilon}(g, \omega) q$  satisfies the following dual weak form*

$$(19) \quad \int_{\Gamma} \int_D \left( \alpha(x, \omega) \nabla y \nabla v + \frac{1}{\epsilon} (1 - H_{\epsilon}(g)) y v \right) dx dP = \frac{1}{\epsilon} \int_{\Gamma} \int_D H'_{\epsilon}(g) q u_{\epsilon} v dx dP,$$

*where  $X(D)$  is a functional space in  $D$ .*

*Proof.* For fixed  $g, q \in X(D)$  and  $\delta \neq 0$ , let  $u_{\epsilon}^{\delta}(\omega) = u_{\epsilon}(g + \delta q, \omega)$ ,  $u_{\epsilon}(\omega) = u_{\epsilon}(g, \omega)$  are solutions of (11) corresponding to the parameter  $g + \delta$  and  $g$ , separately. For any  $v \in L^2(\Gamma; H_0^1(D))$ , subtracting the state equations under the parameters  $g + \delta q$  and  $g$ , we get

$$\int_{\Gamma} \int_D \alpha(x, \omega) \nabla (u_{\epsilon}^{\delta} - u_{\epsilon}) \nabla v dx dP + \frac{1}{\epsilon} \int_{\Gamma} \int_D \left[ (1 - H_{\epsilon}(g + \delta q)) u_{\epsilon}^{\delta} - (1 - H_{\epsilon}(g)) u_{\epsilon} \right] v dx dP = 0.$$



Define  $z^\delta := u_\epsilon^\delta(\omega) - u_\epsilon(\omega) \in L^2(\Gamma; H_0^1(D))$ , the above equality can be reformulated by

$$(20) \quad \int_\Gamma \int_D \alpha(x, \omega) \nabla z^\delta \nabla v dx dP + \frac{1}{\epsilon} \int_\Gamma \int_D (1 - H_\epsilon(g + \delta q)) z^\delta v dx dP \\ = \frac{1}{\epsilon} \int_\Gamma \int_D \frac{H_\epsilon(g + \delta q) - H_\epsilon(g)}{\delta} u_\epsilon v dx dP.$$

Choosing  $v = z^\delta$ , it obtains

$$\int_\Gamma \int_D \alpha(x, \omega) |\nabla z^\delta|^2 dx dP + \frac{1}{\epsilon} \int_\Gamma \int_D (1 - H_\epsilon(g + \delta q)) |z^\delta|^2 dx dP \\ = \frac{1}{\epsilon} \int_\Gamma \int_D \frac{H_\epsilon(g + \delta q) - H_\epsilon(g)}{\delta} u_\epsilon z^\delta dx dP.$$

By using the Assumption 2.2, Poincaré inequality, Cauchy-Schwarz inequality, and notice that  $H_\epsilon(g)$  is Lipschitz continuous, we conclude that the sequence  $\{z^\delta\}$  is bounded in  $L^2(\Gamma; H_0^1(D))$ . Therefore, there exists subsequences  $\delta_k \rightarrow 0$  and  $y \in L^2(\Gamma; H_0^1(D))$  such  $z^{\delta_k} \rightarrow y$  is weakly convergent in  $L^2(\Gamma; H_0^1(D))$ , i.e., for any  $\phi \in L^2(\Gamma; H^{-1}(D))$ ,

$$\int_\Gamma \langle \phi(\omega), z^{\delta_k}(\omega) \rangle dP \rightarrow \int_\Gamma \langle \phi(\omega), y(\omega) \rangle dP,$$

and  $y$  is independent of the subsequence  $z^{\delta_k}$ . Hence,  $z^\delta \rightarrow y$  is weakly convergent.

This illustrates the first conclusion.

Let  $\delta \rightarrow 0$  in (20), since  $z^\delta \rightarrow y$  is weakly convergent, then

$$\int_\Gamma \int_D \alpha(x, \omega) \nabla z^\delta \nabla v dx dP + \frac{1}{\epsilon} \int_\Gamma \int_D (1 - H_\epsilon(g + \delta q)) z^\delta v dx dP \\ \rightarrow \int_\Gamma \int_D \alpha(x, \omega) \nabla y \nabla v + \frac{1}{\epsilon} (1 - H_\epsilon(g)) y v dx dP.$$

It is easy to verify that  $\frac{H_\epsilon(g + \delta q) - H_\epsilon(g)}{\delta} u_\epsilon v$  is convergent a.e. in  $\Gamma \times D$  as  $\delta \rightarrow 0$ .

Besides, there exists a function  $G(x, \omega)$  and Lipschitz constant  $L$ , such that

$$\left| \frac{H_\epsilon(g + \delta q) - H_\epsilon(g)}{\delta} u_\epsilon v \right| \leq L \|q\|_{L^\infty(D)} |u_\epsilon| |v| := G(x, \omega).$$

Due to  $u_\epsilon, v \in L^2(\Gamma; L^2(D))$ , it yields the following integrability

$$\int_\Gamma \int_D G(x, \omega) dx dP = L \|q\|_{L^\infty(D)} \|u_\epsilon\|_{L^2(\Gamma; L^2(D))} \|v\|_{L^2(\Gamma; L^2(D))}.$$

By dominated convergence theorem for the right-hand side of (20), we have

$$\frac{1}{\epsilon} \int_\Gamma \int_D \frac{H_\epsilon(g + \delta q) - H_\epsilon(g)}{\delta} u_\epsilon v dx dP \rightarrow \frac{1}{\epsilon} \int_\Gamma \int_D H'_\epsilon(g) q u_\epsilon v dx dP.$$

To sum up, for any  $v \in L^2(\Gamma; H_0^1(D))$ , (19) holds.  $\square$

**Theorem 2.7.** *If the objective functional has the form  $\mathbb{E} [\frac{1}{2} \int_K (u - u_d)^2 dx]$ , and  $g \geq 0$  holds in  $K$ , then its directional derivative equals*

$$(21) \quad \mathbb{E} \left[ \frac{1}{\epsilon} \int_D (H'_\epsilon(g)) q u_\epsilon z dx \right],$$

here,  $z$  is the weak solution of the approximate adjoint equation (16).

*Proof.* Due to the uniqueness of the weak solution of the approximate state equation, by (8)-(10), with the abuse of notations, define the objective functional

$$(22) \quad j(g) = \frac{1}{2} \mathbb{E} \left[ \int_K (u(g) - u_d)^2 dx \right],$$

naturally, for any  $\delta > 0$  and  $q \in X(D)$ ,

$$(23) \quad \begin{aligned} j(g + \delta q) &= \frac{1}{2} \mathbb{E} \left[ \int_K (u(g + \delta q) - u_d)^2 dx \right] \\ &= \frac{1}{2} \mathbb{E} \left[ \int_K |u(g + \delta q) - u(g) + u(g) - u_d|^2 dx \right] \\ &= \frac{1}{2} \mathbb{E} \left[ \int_K |u(g) - u_d|^2 dx \right] + \frac{1}{2} \mathbb{E} \left[ \int_K |u(g + \delta q) - u(g)|^2 dx \right] \\ &\quad + \mathbb{E} \left[ \int_K (u(g + \delta q) - u(g), u(g) - u_d) dx \right], \end{aligned}$$

by using the adjoint equation (16) and Lemma 2.6, we have

$$\begin{aligned} \partial_g j(g) \delta &= \lim_{\delta \rightarrow 0} \frac{j(g + \delta q) - j(g)}{\delta} \\ &= \lim_{\delta \rightarrow 0} \frac{\frac{1}{2} \mathbb{E} \left[ \int_K |u(g + \delta q) - u(g)|^2 dx \right] + \mathbb{E} \left[ \int_K (u(g + \delta q) - u(g), u(g) - u_d) dx \right]}{\delta} \\ &= \lim_{\delta \rightarrow 0} \mathbb{E} \left[ \int_K \frac{(u(g + \delta q) - u(g))^2}{2\delta} dx \right] + \mathbb{E} \left[ \int_K \lim_{\delta \rightarrow 0} \frac{u(g + \delta q) - u(g)}{\delta} (u(g) - u_d) dx \right] \\ &:= I + II, \end{aligned}$$

For term  $I$ , Lemma 2.6 tells us  $\{z^\delta\}$  is uniformly bounded in  $L^2(\Gamma; L^2(D))$ , i.e., there is a constant  $C$  satisfies  $\sup_{\delta} \mathbb{E} [\|z^\delta\|_{L^2(D)}] \leq C$ , this equivalents

$$\left| \mathbb{E} \left[ \int_K \frac{(u(g + \delta q) - u(g))^2}{2\delta} dx \right] \right| \leq \mathbb{E} \left[ \frac{\delta}{2} \|z^\delta\|_{L^2(D)} \right] \leq \frac{\delta}{2} C,$$

Naturally,  $I = 0$  and  $II = \mathbb{E} [\int_K y(u(g) - u_d)]$ . In (16), let  $v = y \in L^2(\Gamma; H_0^1(D))$ , then in virtue of (19) with  $v = z$ , we obtain

$$\mathbb{E} [y(u(g) - u_d) dx] = \frac{1}{\epsilon} \mathbb{E} \left[ \int_D H'_\epsilon(g) q u_\epsilon z dx \right].$$

Consequently,  $\partial_g j(g) \delta = \frac{1}{\epsilon} \mathbb{E} [\int_D H'_\epsilon(g) q u_\epsilon z dx]$ , the proof is finished.  $\square$

## 3. PROPOSED ALGORITHM

In this section, we first mainly focus on the discretization method (FEM) on physical space, and then use Monte Carlo approximation (MC) to deal with random variable. Lastly, an accelerated version of gradient descent method (AGD) is adopted to update  $g$ .

**3.1. FEM discretization.** For applying FEM, we consider a family of triangulations  $\{\mathcal{T}_h\}_{h>0}$  consist of triangles  $T$  which satisfy  $\bar{D} = \bigcup_{T \in \mathcal{T}_h} T$ , and suppose all the triangulations used in this paper are shape regular. Here  $h$  stands for the maximal diameter of all triangles  $T$ . With the triangulation  $\{\mathcal{T}_h\}_{h>0}$ , define the finite element spaces

$$\begin{aligned} V_h &= \{v_h \in H^1(D) \mid v_h|_T \in \mathbb{P}_1, \forall T \in \mathcal{T}_h\}, \\ V_h^0 &= \{v_h \in H_0^1(D) \mid v_h|_T \in \mathbb{P}_1, \forall T \in \mathcal{T}_h\}, \end{aligned}$$

and the approximation sets of  $U$  and  $F$  could be defined as:

$$U_h = L^2(\Gamma; V_h^0), \quad F_h = V_h,$$

where  $\mathbb{P}_1$  is the space of polynomials of degree less than or equal to 1.

Further, let  $\Phi = \Phi(x) = (\phi_1(x), \dots, \phi_N(x))$  denotes a vector valued function consisting of all the basis functions of  $V_h$ , where  $N$  stands for the number of basis function (or degree of freedom). For any fixed  $\omega \in \Gamma$ , the vector  $\mathbf{u}_\epsilon(\omega) = (u_1(\omega), \dots, u_N(\omega))^T \in \mathbb{R}^N$ , then the FEM approximations of the state variable  $u_\epsilon$  and the control variable  $f$  could be written as

$$u_h(x, \omega) = \sum_{j=1}^N u_j(\omega) \phi_j(x) \in U_h, \quad f_h(x) = \sum_{j=1}^N f_j \phi_j(x) \in F_h,$$

where  $\{\phi_j\}_{j=1}^N$  stands for basis functions of  $U_h$ , and  $N$  represents the degree of freedom on  $D$ . Replacing  $u_h$  and  $f_h$  by  $\Phi \mathbf{u}_\epsilon(\omega)$  and  $\Phi \mathbf{f}$ , so (11) can be reformulated by

$$(24) \quad A(\omega_i) \mathbf{u}_\epsilon(\omega_i) = B_1 \mathbf{f}, \quad i = 1, \dots, M,$$

here,

$$(25) \quad \begin{aligned} A(\omega_i) &= (\alpha(x, \omega_i) \nabla \phi_m, \nabla \phi_n)_{L^2(D)} + \frac{1}{\epsilon} ((1 - H_\epsilon(g)) \phi_m, \phi_n)_{L^2(D)} \in \mathbb{R}^{N \times N}, \\ B_1 &= (\phi_m, \phi_n)_{L^2(D)} \in \mathbb{R}^{N \times N}. \end{aligned}$$

Similarly, if the cost functional satisfies (15), then the matrix-vector form of (16) is

$$(26) \quad A(\omega_i)\mathbf{z}(\omega_i) = B_2(\mathbf{u}_\epsilon - \mathbf{u}_d), \quad i = 1, \dots, M,$$

with  $B_2 = ((1 - H_\epsilon(g))\phi_m, \phi_n)_{L^2(D)} \in \mathbb{R}^{N \times N}$ , or equivalently, the right-hand side of (26) is  $B_3(u_\epsilon - u_d)$  with  $B_3 = (\phi_m, \phi_n)_{L^2(O)}$ .

**3.2. MC approximation and gradient descent method.** In this subsection, we mainly apply the standard MC method to approximate the expectation operator  $\mathbb{E}$ .  $\{\omega_i\}_{i=1}^M$  ( $M \gg 1$ ) are the identically distributed independent samples chosen from the probability space  $(\Gamma, \mathcal{F}, P)$ . Because of the law of large numbers and the central limit theorem, for any state variable  $u \in L^2(\Gamma; H^1(D))$ , we can approximate the expectation  $\mathbb{E}[u_h(x, \omega)]$  by the average of the  $M$  samples

$$(27) \quad \mathbb{E}_M[u_h(x, \omega)] = \frac{1}{M} \sum_{i=1}^M u_h(x, \omega_i),$$

After FEM and MC, we can derive the following discretized shape optimization objective functional

$$(28) \quad \min_g E_{M,h} \left[ \int_{\Omega} J(x, \omega, u_h(x, \omega)) dx \right]$$

In the following, an accelerated version of gradient descent method is used to solve the above optimal problem and update the parameter  $g$ . Now, we can describe the update process in the following algorithm.

**Algorithm 1** FEM-MC-AGD

---

**Input:** Initial shape function  $\mathbf{g}^0$ , positive step sizes  $\alpha_0$ , random sample set  $\{\omega_i\}_{i \geq 1}$ , force term  $f$ , desired state  $u_d$  and regularization parameter  $\epsilon$ ,  $k = 0$ ;

**Output:** the optimal shape related to  $\mathbf{g}^{k+1}$ ;

- 1: Generate constant mass matrix  $B_1$ ;
- 2: **while** not stopping condition **do**
- 3:   **for all**  $i = 1, 2, \dots, M$  **do**
- 4:     Generate the stochastic approximate stiffness matrix  $A(\omega_i)$ , compute the solution vector  $\mathbf{u}_\epsilon^k(\omega_i)$  of primal equation by (24);
- 5:     Compute the cost value  $j(\mathbf{g}^{k+1})$ ;
- 6:     Generate the approximate mass matrix  $B_2$ , compute the solution vector  $\mathbf{z}^k(\omega_i)$  of dual equation (if (15) holds, then by (26));
- 7:     Compute the stochastic gradient vector  $\nabla j(\mathbf{g}^k)$  by using  $\mathbf{u}_\epsilon^k(\omega_i)$ ,  $\mathbf{z}^k(\omega_i)$ ;
- 8:   **end for**
- 9:   Compute the average gradient  $\nabla \bar{j}(\mathbf{g}^k)$  and the average cost  $\bar{j}(\mathbf{g}^{k+1})$ ;
- 10:   Update  $\mathbf{g}^{k+1} = \mathbf{g}^k - \alpha_k \nabla \bar{j}(\mathbf{g}^k)$ , where  $\alpha_k$  satisfy Armijo condition;
- 11:    $k = k + 1$ ;
- 12: **end while**

---

**Remark 3.1.** In the above algorithm, the stopping condition include setting the maximum iteration steps,  $k = 1, 2, \dots, K_{max}$ , using the relative (absolute) error between  $\mathbf{g}^k, \mathbf{g}^{k+1}$  or  $j(\mathbf{g}^k), j(\mathbf{g}^{k+1})$ . For example, we stop the algorithm if  $|j(\mathbf{g}^{k+1}) - j(\mathbf{g}^k)| < 1e - 8$  or  $\|\mathbf{g}^{k+1} - \mathbf{g}^k\|_2 < 1e - 8$  holds, where  $\frac{\|\mathbf{g}^{k+1} - \mathbf{g}^k\|_2}{\|\mathbf{g}^{k+1}\|_2}$  is used instead of  $\|\mathbf{g}^{k+1} - \mathbf{g}^k\|_2$  if  $\|\mathbf{g}^{k+1}\|_2 \geq 1$ , and analogous for  $j(\mathbf{g}^k)$  using absolute value to measure.

**Remark 3.2.** When considering objective functional (18) and  $O \subset K \subset D$ , we need to project the solution into the domain  $K$  because constraint  $g \geq 0$  has been imposed on this set.

**Remark 3.3.** An enhanced search scheme—three-point quadratic interpolation coupled with quadratic fitting method is applied to search for the optimal step size in gradient descent method. More specifically, it evaluates cost at three strategically chosen points relative to the historical step size:  $[0.5\alpha_{prev}, \alpha_{prev}, 1.5\alpha_{prev}]$ , then fits a quadratic polynomial to the cost values and computes the exact minimum. We also set the minimum, maximum step size  $\alpha_{min} = 1, \alpha_{max} = 10$ , separately.

*In the iteration process, momentum gradient smoothing is also used to accelerate convergence, which combines current gradient with historical information.*

#### 4. NUMERICAL EXPERIMENTS

The purpose of this section is to illustrate the validity and main features from the previous sections with the propose four numerical examples.

We consider the optimization shape problem on the spatial domain  $D = (-1, 1)^2 \subset \mathbb{R}^2$ , the diffusion coefficient  $\alpha(x, \omega)$  is set to be

$$(29) \quad \alpha(x, \omega) = 1 + \rho\eta(x, \omega),$$

other cases could be considered similarly. Here,  $\rho = 0.01$  stands for the disturbing degree,  $\eta(x, \omega) \in L^2(\Gamma; L^\infty(D))$  denotes the random process satisfying

$$\mathcal{P}\{\omega \in \Gamma; \|\eta(x, \omega)\|_{L^\infty(D)} \leq 1\} = 1,$$

and obeys the uniform distribution on the interval of  $[-1, 1]$  for any fixed  $x \in D$ . Fixed regularization parameter  $\epsilon = 1e - 5$ , the maximum iteration steps  $K_{max} = 1000$  and sample number  $M = 100$ . Considering the samples are independent and identify distribution and the structure of the algorithms, we adopt a parallel strategy to accelerate the running speed. In addition, we observe  $H_\epsilon(g)$  is a monotone increasing function, so the simplified gradient which drop the term  $H'_\epsilon(g)$  can be applied to the algorithm, this will reduce the computation. The finite element mesh size  $h = \frac{1}{128}$ , including 32258 triangular elements and 16384 vertices.

**Example 4.1.** *In this example, we consider the objective functional*

$$j(x, \omega, u(x, \omega)) = \frac{1}{2} \mathbb{E} \left[ \int_O (u - u_d)^2 dx \right]$$

*with  $u_d(x) = -(x_1 - \frac{1}{2})^2 - (x_2 - \frac{1}{2})^2 + \frac{1}{8}$  and the fixed square domain  $O = [-\frac{1}{2}, \frac{1}{2}]^2 \subset D$ . The initial shape function is*

$$g^0(x) = \frac{7}{8} - x_1^2 - x_2^2,$$

*the right-hand side function  $f = 2$ . Besides, we impose the extra constraint  $g \geq 0$  in  $O$ . In the algorithm, the simplified descent direction is the negative gradient direction  $d = -\frac{1}{\epsilon} \mathbb{E}[u_\epsilon z]$ .*

Figure 1 shows the initial geometry with the boundary, where the solid blue line represents the boundary of  $g^0(x)$ , the black dotted line represents area  $D$  and

the dotted line in magenta indicates the boundary of area  $O$ , while the optimal geometry is none other than the square domain  $O$ .

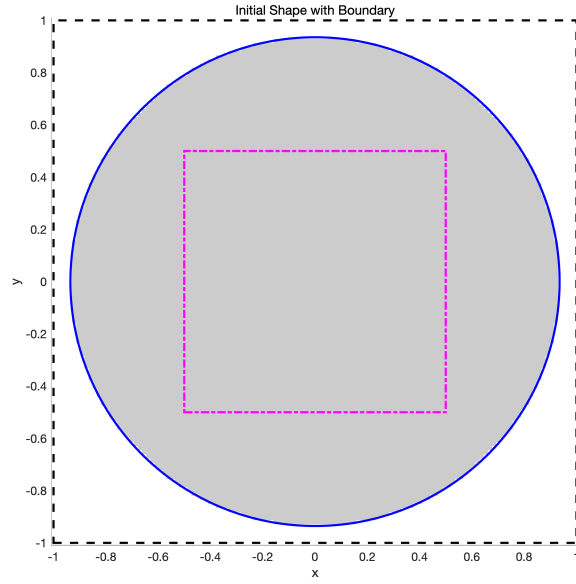


FIGURE 1. The initial shape with boundary.

Figure 2 indicates some intermediate shape during iteration, the corresponding expected cost values are 0.475400, 0.269463, 0.265508, 0.265508, 0.265507, 0.265507. In the last step, the absolute change of the costs  $|j(\mathbf{g}^{k+1}) - j(\mathbf{g}^k)|$  is  $2.1103e - 10$ , and the corresponding expected cost is 0.265507. We also present the iterative variation curve of the expected cost in Figure 3.

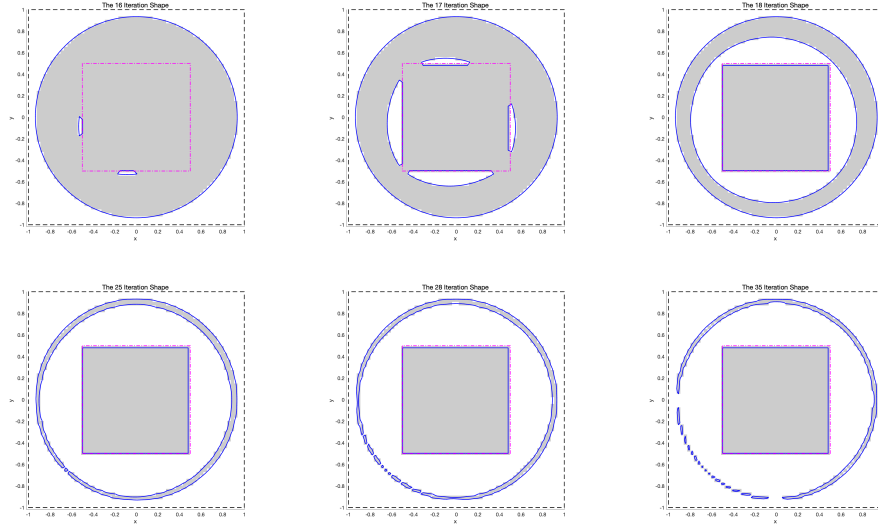


FIGURE 2. The iterative shapes with boundary of steps 16, 17, 18, 25, 28 and 35.

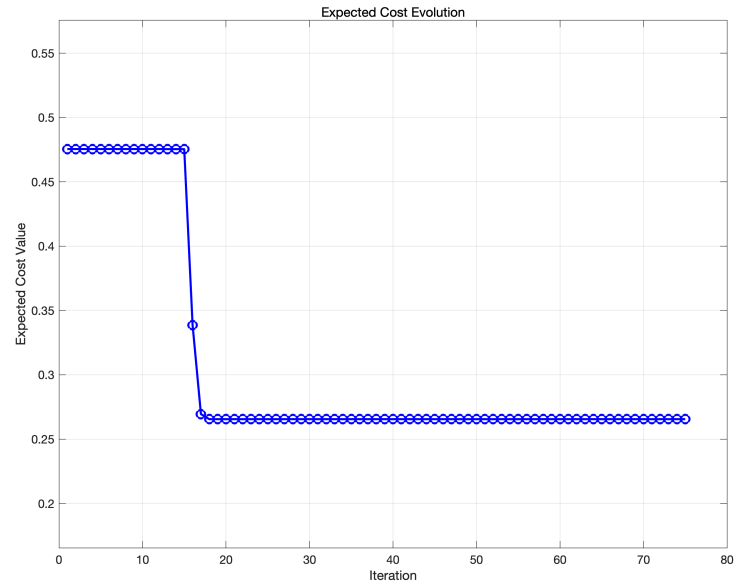


FIGURE 3. The variations of expected cost cure with iterations of Example 4.1.



**Example 4.2.** Based on Example 4.1, and now let the force term is a function depend on the spatial coordinate, that is  $f(x) = 2\pi^2 \sin(\pi x_1) \sin(\pi x_2) + 1$ , and  $u_d = \sin(\pi x_1) \sin(\pi x_2)$ .

We show some intermediate geometries for shape optimizations using the same initial shape as Example 4.1. We observe that the intermediate iteration shape and the final shape are different from the previous example. Hence, the square area  $O$  is the theoretical optimal shape. We also notice that the shape update starts from the upper right corner and the lower left corner, it has central symmetry, these symmetries are visible in Figure 4. Figure 5 shows the expected cost evolution, in this example, the cost value at the final step of the iteration is 0.163355, the absolute change of cost value  $|j(\mathbf{g}^{k+1}) - j(\mathbf{g}^k)|$  is  $9.6571e - 10$  and the relative change  $\frac{\|\mathbf{g}^{k+1} - \mathbf{g}^k\|_2}{\|\mathbf{g}^{k+1}\|_2}$  is  $1.3943e - 04$ .

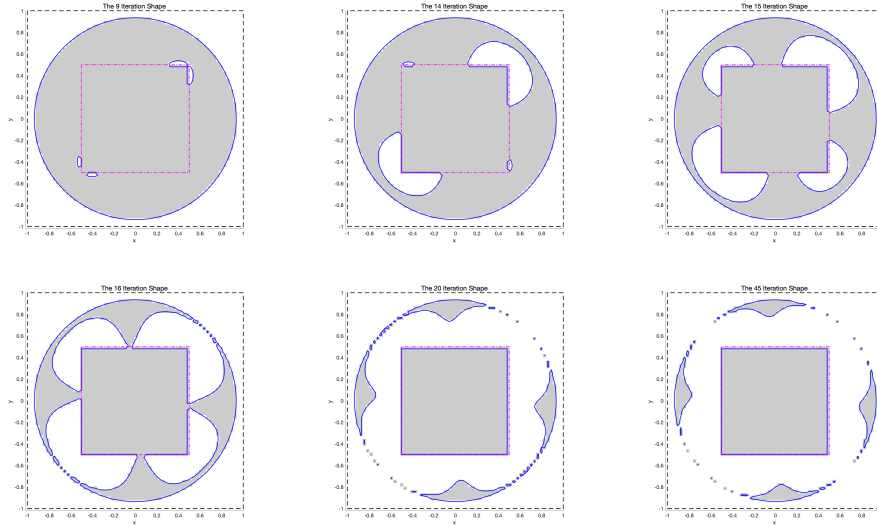


FIGURE 4. The iterative shapes with boundary of steps 9, 14, 15, 16, 20, and 45.

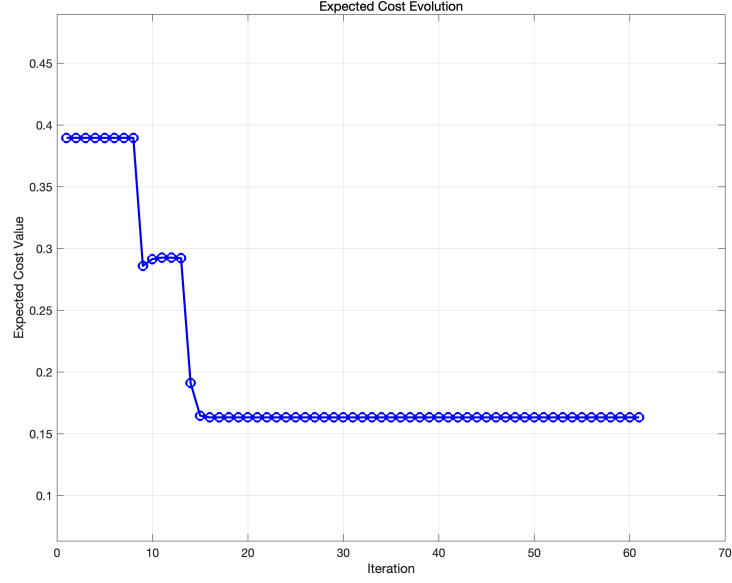


FIGURE 5. The variations of expected cost cure with iterations of Example 4.1.

**Example 4.3.** *In this example, we only modify the subdomain  $O$  to a disk area with the center at  $(0,0)$  and a radius of  $\frac{1}{2}$ , other parameter settings are same with Example 4.2.*

The graphical representation about expected cost evolution is shown in Figure 6. Figure 7 shows the expected cost evolution, In this example, the variation accuracy order of cost absolute value  $|j(\mathbf{g}^{k+1}) - j(\mathbf{g}^k)|$  can also achieve  $1e - 10$ , and the final expected cost is 0.065557.

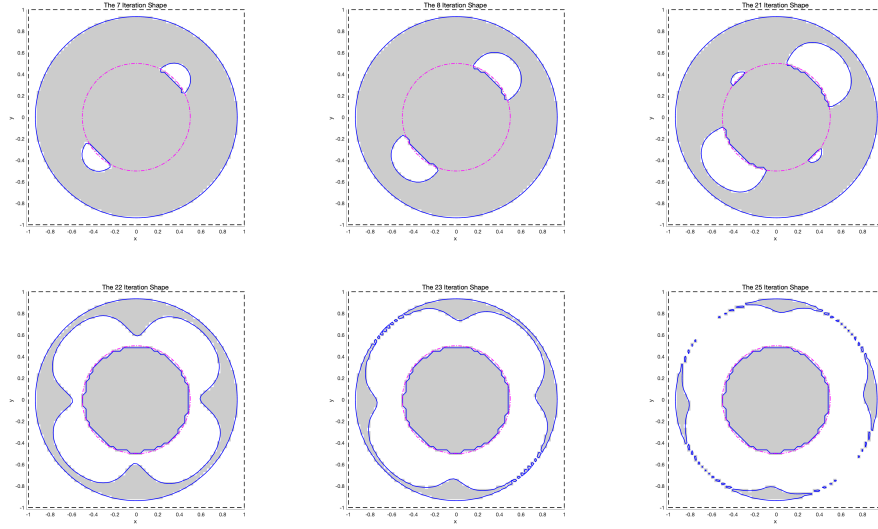


FIGURE 6. The iterative shapes with boundary of steps 7, 8, 21, 22, 23 and 25.

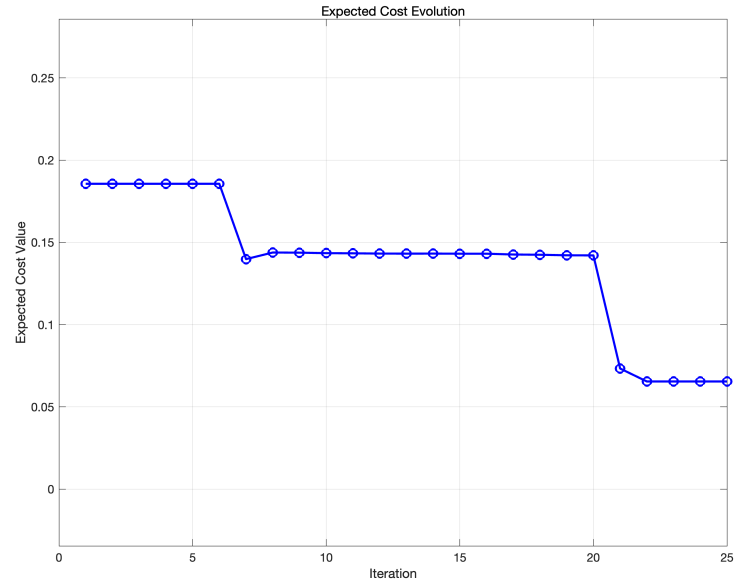


FIGURE 7. The variations of expected cost cure with iterations of Example 4.2.

From the first three examples, it can be seen that regardless of whether region  $O$  is a square region or a circular region, and regardless of whether the right-hand term is a constant function or not, the final shape basically satisfies the theory that  $O$  is the optimal shape, with only a small noise disturbance at the boundary. It can be seen from the change process that the shape change in the later stage of the iteration is relatively small.

**Example 4.4.** *For this example, we use a different objective functional, we restrict the integral domain is  $K$ , that is*

$$(30) \quad j(x, \omega, u(x, \omega)) = \frac{1}{2} \mathbb{E} \left[ \int_K (u - u_d)^2 dx \right]$$

with  $u_d = -(x_1 - \frac{1}{4})^2 - (x_2 - \frac{1}{4})^2 + \frac{1}{25}$ , or, equivalently, the objective functional is

$$j(x, \omega, u(x, \omega)) = \frac{1}{2} \mathbb{E} \left[ \int_D H_\epsilon(g) (u - u_d)^2 dx \right].$$

The initial shape function is

$$g^0(x) = \min \left\{ 1 - (x_1^2 + x_2^2), x_1^2 + x_2^2 - \frac{1}{64}, (x_1 - \frac{1}{2})^2 + x_2^2 - \frac{1}{16} \right\},$$

the force function  $f = 2$  and the restriction  $g \geq 0$  in  $O$  is not imposed. In the algorithm, we use the reduced descent direction  $d = -\mathbb{E} \left[ \frac{1}{2} (u_\epsilon - u_d)^2 + \frac{1}{\epsilon} u_\epsilon z \right]$ .

We first show the initial shape in Figure 8.

Then geometries of the intermediate step iteration are illustrated in Figure 9, where the gray area stands for the region  $g \geq 0$ , blue line denotes the boundary  $g = 0$  and the cavity is the region  $g \leq 0$ . Figure 10 show the evolution process of expected costs with iterations. When the algorithm stops, the final absolute change of cost value  $|j(\mathbf{g}^{\mathbf{k}+1}) - \mathbf{j}(\mathbf{g}^{\mathbf{k}})|$  is  $9.1697e - 13$ , and the expected cost value is  $3.5e - 5$ . Actually, from the objective form, we can get the conclusion that the optimal shape is the empty set. From the perspective of the evolution process of shape, they are evolving towards an empty set.

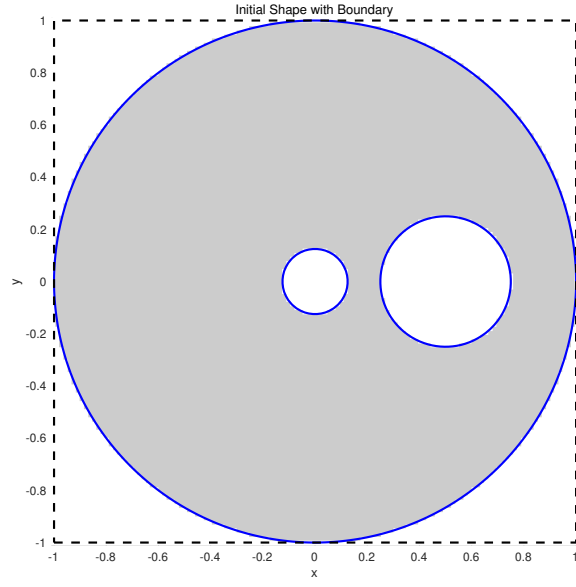


FIGURE 8. The initial shape with boundary of Example 4.4.

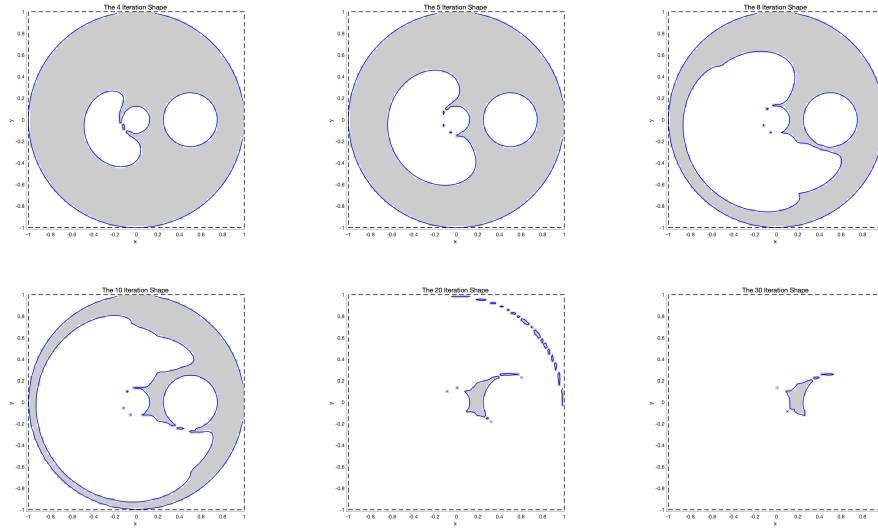


FIGURE 9. The iterative shapes with boundary of steps 4, 5, 8, 10, 20 and 30.

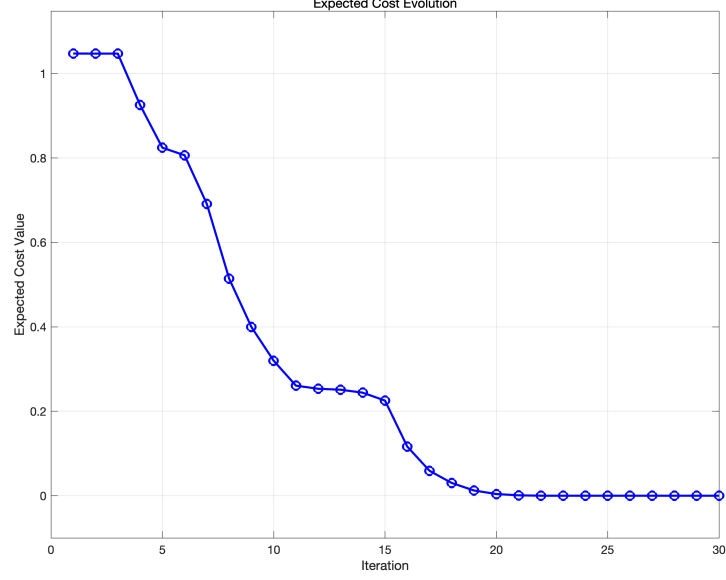


FIGURE 10. The variations of expected cost cure with iterations of Example 4.4.

## 5. CONCLUSION

This paper presents an efficient discretize-then-optimize framework for elliptic PDE-constrained stochastic shape optimization with random diffusion coefficients. Element-wise stochasticity creates high-frequency noise requiring finite element method coupled with Monte Carlo method, where Monte Carlo method is applied to parallel compute the samples information. While demonstrated on diffusion-based shape optimization, our approach can extend to any PDE-constrained optimization with uncertain parameters.

## ACKNOWLEDGEMENTS

The author would like to thank Professor Tiba Dan for helpful discussions and supports to the completion of this paper. The work of X. Pang was supported by Science Foundation of Hebei Normal University No. L2022B30 and China Scholarship Council No. 202308130193. The whole work was also funded by the Natural Science Foundation of Hebei Province No. A2023205045.

## REFERENCES

- [1] P. Antonietti, A. Borzí and M. Verani. Multigrid shape optimization governed by elliptic PDEs, *SIAM J. Control Optim.*, 2013, 51(2): 1417–1440.
- [2] G. Allaire and C. Dapogny. A deterministic approximation method in shape optimization under random uncertainties. *SMAI J. Comput. Math.*, 2015, 1: 83–143.
- [3] R. Adams and J. Fournier. Sobolev spaces. Academic press, Oxford, 2003.
- [4] B. Bogosel. Numerical shape optimization among convex sets. *Appl. Math. Optim.*, 2023, 87(1): 1–31.
- [5] A. Chakib, I. Khalil and A. Sadik. An improved numerical approach for solving shape optimization problems on convex domains. *Numer. Algorithms*, 2024, 96(2): 621–663.
- [6] S. Chen, W. Chen and S. Lee. Level set based robust shape and topology optimization under random field uncertainties. *Struct. Multidiscip. Optim.*, 2010, 41(4): 507–524.
- [7] S. Conti, H. Held, M. Pach, Martin Rumpf, and R. Schultz. Risk averse shape optimization. *SIAM J. Control Optim.*, 2011, 49(3): 927–947.
- [8] M. Dambrine, Charles Dapogny and H. Harbrecht. Shape optimization for quadratic functionals and states with random right-hand sides. *SIAM J. Control Optim.*, 2015, 53(5): 3081–3103.
- [9] W. Gong, J. Li and S. Zhu. Improved discrete boundary type shape gradients for PDE-constrained shape optimization. *SIAM J. Sci. Comput.*, 2022, 44(4): A2464–A2505.
- [10] C. Geiersbach, E. Loayza-Romero, and K. Welker. PDE-constrained shape optimization: toward product shape spaces and stochastic models. *Handbook of mathematical models and algorithms in computer vision and imaging—mathematical imaging and vision*, Springer, 2023, 1585–1630.
- [11] Q. Guan, X. Guo, and W. Zhao. Efficient numerical method for shape optimization problem constrained by stochastic elliptic interface equation. *Commun. Anal. Comput.*, 2023, 1(4): 321–346.
- [12] C. Geiersbach and G. Pflug. Projected stochastic gradients for convex constrained problems in Hilbert spaces. *SIAM J. Optim.*, 2019, 29 (3):2079–2099.
- [13] H. Harbrecht. On output functionals of boundary value problems on stochastic domains. *Math. Methods Appl. Sci.*, 2010, 33 (1): 91–102.
- [14] M. Hinze, R. Pinnau, M. Ulbrich and S. Ulbrich. Optimization with PDE constraints. Springer Verlag, 2010.
- [15] H. Kasumba, G. Kakuba and J. Mango. A second order fixed domain approach to a shape optimization problem. *Progress in industrial mathematics at ECMI*, 2016, 657–663, *Math. Ind. Eur. Consort. Math. Ind. (Berl.)*, 26 , Springer.
- [16] Z. Luo, M. Wang, S. Wang and P. Wei. A level set-based parameterization method for structural shape and topology optimization. *Internat. J. Numer. Methods Engrg.*, 2008, 76 (1): 1–26.

- [17] J. Martínez-Frutos, M. Kessler and F. Periago. Robust optimal shape design for an elliptic PDE with uncertainty in its input data. *ESAIM Control Optim. Calc. Var.*, 2015, 21 (4): 901–923.
- [18] J. Martínez-Frutos, D. Herrero-Pérez, M. Kessler and F. Periago. Robust shape optimization of continuous structures via the level set method. *Comput. Methods Appl. Mech. Engrg.*, 2016, 305: 271–291.
- [19] J. Martínez-Frutos, D. Herrero-Pérez, M. Kessler and F. Periago. Risk-averse structural topology optimization under random fields using stochastic expansion methods. *Comput. Methods Appl. Mech. Engrg.*, 2018, 330: 180–206.
- [20] C. Murea and D. Tiba. Topological optimization via cost penalization, *Topol. Methods Non-linear Anal.*, 2019, 54(2B): 1023–1050.
- [21] P. Neittaanmäki, J. Sprekels and D. Tiba. *Optimization of elliptic systems. Theory and Applications*, Springer, 2006.
- [22] P. Neittaanmäki and D. Tiba. A fixed domain approach in shape optimization problems with Neumann boundary conditions. *Partial Differential Equations. Modelling and Numerical Simulation, Comput. Methods Appl. Sci.*, 2008, 16: 235–244.
- [23] P. Neittaanmäki, A. Pennanen and D. Tiba. Fixed domain approaches in shape optimization problems with Dirichlet boundary conditions. *Inverse Problems*, 2009, 25, 055003(18pp).
- [24] O. Pironneau. *Optimal shape design for elliptic systems*. Springer, New York, 1984.
- [25] P. Philip and D. Tiba, A penalization and regularization technique in shape optimization problems, *SIAM J. Control Optim.*, 2013, 51(6): 4295–4317.
- [26] P. Philip and D. Tiba, Shape optimization via control of a shape function on a fixed domain: theory and numerical results. *Numerical methods for differential equations, optimization, and technological problems*, 2013, 305–320, *Comput. Methods Appl. Sci.*, 27, Springer.
- [27] J. De los Reyes. *Numerical PDE-constrained optimization*. Springer, 2015.
- [28] S. Schmidt, C. Ilic, V. Schulz and N.R. Gauger. Three-dimensional large-scale aerodynamic shape optimization based on shape calculus. *AIAA J.*, 2013, 51: 2615–2627.
- [29] F. Tröltzsch. *Optimal control of partial differential equations theory, methods, and applications*. Springer, 2010.
- [30] R. Udawalpola and M. Berggren. Optimization of an acoustic horn with respect to efficiency and directivity. *Internat. J. Numer. Methods Engrg.*, 2008, 73(11): 1571–1606.
- [31] X. Wang, P. Yin, B. Zhang and C. Yang. AONN-2: An adjoint-oriented neural network method for PDE-constrained shape optimization. *J. Comput. Phys.*, 2024, 513, No. 113160, 16 pp.

DEPARTMENT OF MATHEMATICS, HEBEI NORMAL UNIVERSITY, SHIJIAZHUANG, HEBEI, CHINA.

HEBEI KEY LABORATORY OF COMPUTATIONAL MATHEMATICS AND APPLICATIONS, HEBEI.